Theoretical Interpretation of Conductivity Measurements of a Thiotolane Sandwich. A Molecular Scale Electronic Controller

Jorge M. Seminario,* Angelica G. Zacarias, and James M. Tour*

Contribution from the Department of Chemistry and Biochemistry, University of South Carolina, Columbia, South Carolina 29208

Received October 20, 1997. Revised Manuscript Received March 4, 1998

Abstract: Quantum density functional theory and classical molecular dynamics studies of tolane molecules are carried out to interpret results of conductivity measurements on a monolayer of thiotolane molecules self-assembled on a gold surface and sandwiched by a titanium layer. Density functional theory techniques have been used to determine the ground state conformations and electronic structure, while classical molecular dynamics accounts for the effects of pressure and temperature for a cluster of five thiotolane molecules arranged between titanium and gold surfaces used to simulate the experimental system. On the basis of the theoretical results, it can be concluded, in agreement with the experimental findings, that the relative angle between two benzene rings in each tolane molecule determines its conductivity, with a maximum at 0° and a minimum at 90°. Therefore, this system would work as an unbiased controller, where the current through the molecule is controlled by the angle of one phenyl ring with respect to the other.

1. Introduction

Present developments in theoretical and experimental techniques have triggered enormous possibilities of using organic chemistry as a fundamental complement to silicon in semiconductors.[1] This may allow the fabrication of logical circuits at the level of single molecules.[2] Further advances in this area require precise knowledge of the effects of crossing electrons over target organic molecules. One of the major class of compounds used for conductivity studies is thiol-terminated conjugated oligomers because of the possibility of constructing self-assembled monolayers (SAMs) that can be used for measurements of electronic transport.[1] The initial goal of previous studies on these compounds was to investigate their potential use as molecular wires.[1,3] This work shows that, in addition to wire-like properties, this class of phenylene−ethynylene oligomers can behave as real full current controllers because the electronic transport properties vary significantly based on the molecular conformations. The current in tolane, one of the smallest conjugated oligomers, is controlled by the angle between its two phenyl rings. This computational study rationalizes the experimental results obtained on these molecules in a nanopore when sandwiched between gold and titanium electrodes.[4]

2. Theory

Density functional theory (DFT) techniques[5−11] were used for the tolane systems. The functionals used are Perdew-Wang 91 for correlation and Becke-3 for exchange (B3PW91).[12−15] The basis set used was the triply split-valence with polarization functions, 6-311G**.[16−18] When the gold clusters are included in the calculations, we combined the above methods with effective core potentials.[19] Presently, this seems to be the most powerful combination of tools to deal with relatively large numbers of very heavy atoms. The basis set used for the gold atom is the Los Alamos National Laboratory (LANL) set for effective core potentials (ECP) of double-ζ type.[20−22] The use

---

* Authors to whom correspondence should be addressed.

[1] (a) Bumm, L. A.; Arnold, J. J.; Cygan, M. T.; Dunbar, T. D.; Burgin, T. P.; Jones, L., II; Allara, D. L.; Tour, J. M.; Weiss, P. S. *Science* **1996**, *271*, 1705−1707. (b) Jones, L., II; Schumm, J. S.; Tour, J. M. *J. Org. Chem.* **1997**, *62*, 1388−1410. (c) Reed, M. A.; Zhou, C.; Muller, C. J.; Burgin, T. P.; Tour, J. M. *Science* **1997**, *278*, 252−254.

[2] Wu, R.; Schumm, J. S.; Pearson, D. L.; Tour, J. M. *J. Org. Chem.* **1997**, *61*, 6906-6921.

[3] Samanta, M. P.; Tian, W.; Datta, S.; Henderson, J. I.; Kubiak, C. P. *Phys. Rev. B* **1996**, *53*, R7626−R7629.

[4] For an analogous study on biphenylthiol sandwiched between Au and Ti electrodes in a nanopore junction see: Zhou, C.; Deshpande, M. R.; Reed, M. A.; Jones, L., II; Tour, J. M. *Appl. Phys. Lett.* **1997**, *71*, 611−613. More recent experimental results have been obtained for thiotolane and they will be published separately.

[5] Seminario, J. M.; Politzer, P., Eds.; *Modern Density Functional Theory: A Tool for Chemistry*; Elsevier: Amsterdam, 1995; p 405.

[6] Seminario, J. M., Ed. *Recent Developments and Applications of Modern Density Functional Theory*; Elsevier: Amsterdam, 1996; p 900.

[7] Chong, D. P., Ed. *Recent Advances in Density Functional Theory (Part I)*; World Scientific: Singapore, 1995; p 413.

[8] Parr, R. G.; Yang, W. *Density Functional Theory of Atoms and Molecules*; Oxford University Press: Oxford, 1989.

[9] Kryachko, E. S.; Ludeña, E. *Energy Density Functional Theory of Many-electron Systems*; Academic: New York, 1990.

[10] Dreizler, R. M.; Gross, E. K. U. *Density Functional Theory*; Springer-Verlag: Berlin, 1990.

[11] Labanowski, J. K.; Andzelm, J. W., Eds.; *Density Functional Methods in Chemistry*; Springer: New York, 1991; p 443.

[12] Becke, A. D. *J. Chem. Phys.* **1993**, *98*, 5648−5652.

[13] Perdew, J. P. In *Electronic Structure of Solids*; Ziesche, P., Eschrig, H., Eds.; Akademie Verlag: Berlin, 1991; pp 11−20.

[14] Perdew, J. P.; Chevary, J. A.; Vosko, S. H.; Jackson, K. A.; Pederson, M. R.; Singh, D. J.; Fiolhais, C. *Phys. Rev. B* **1992**, *46*, 6671−6687.

[15] Perdew, J. P.; Wang, Y. *Phys. Rev. B* **1992**, *45*, 13244−13249.

[16] Hay, P. J. *J. Chem. Phys.* **1977**, *66*, 4377−4384.

[17] Raghavachari, K.; Trucks, G. W. *J. Chem. Phys.* **1989**, *91*, 1062−1065.

[18] Wachters, A. J. H. *J. Chem. Phys.* **1970**, *52*, 1033−1036.

[19] Dunning, T. H., Jr.; Hay, P. J. In *Modern Theoretical Chemistry*; Shaefer, H. F., III, Ed.; Plenum: New York, 1976; pp 1−28.

[20] Hay, P. J.; Wadt, W. R. *J. Chem. Phys.* **1985**, *82*, 270−283.

[21] Wadt, W. R.; Hay, P. J. *J. Chem. Phys.* **1985**, *82*, 284−298.

S0002-7863(97)03639-1 CCC: $15.00

Table 1. Optimized Geometries and Relative Energies for Three Conformations and Ions of the Tolane Molecule (at 0°, 45°, and 90° between the Phenyl Planes) using the B3PW91/6-311G** Level of Theory (1 $E_h = 627.509$ kcal/mol)

	1a	**1b**	**1c**
	0° D_{2h} ^1A_g	45° D_2	90° D_{2d} $^1A_1$
neutral			
energy (kcal/mol)	0.00	0.41	0.86
HOMO (kcal/mol)	−139.8	−142.5	−150.5
LUMO (kcal/mol)	−37.3	−34.1	−24.8
negative			
energy (kcal/mol)	0.00	3.34	12.02
EA (kcal/mol)	6.3	3.34	−4.89
positive			
energy (kcal/mol)	0.00		14.18
IP (kcal/mol)	173.4		186.75

of DFT is fully justified due to the fact that it is an ab initio tool able to deal with a broad variety of systems. Several successful applications using the hybrid functionals have been reported, where a portion of the exchange functional is calculated as a fully nonlocal functional of the wave function of an auxiliary noninteracting system of electrons. Since this resembles the exchange in the Hartree−Fock (HF) procedure (actually in any wave function procedure), it is common to refer to this functional or procedure as a DFT-HF hybrid. However, it should be considered that the so-called exchange is being calculated by using a noninteractive wave function whose density, but not its wave function, corresponds to the real system. A detailed analysis and their theoretical rigor was recently reviewed.[23] All calculations were performed with the Gaussian-94 program.[24] All geometry optimizations were performed via the Berny algorithm in redundant internal coordinates.[25] The threshold for convergence was 0.00045 and 0.0003 au for the maximum force and root-mean-square force, respectively. The self-consistency of the noninteractive wave function was performed with a requested convergence on the density matrix of 10^{-8}, and 10^{-6} for the RMS and maximum density matrix error between iterations. Within the model chemistry used, these settings provide correct energies of at least five decimal figures and geometries of an accuracy of around three decimal figures. On the other hand, the use of the pseudopotentials with relativistic corrections has been widely demonstrated to be a good compromise with the alternative use of full-electron procedures. This reduces the required computational effort without loss of accuracy.[26]

3. Results and Discussion

Table 1 shows the optimized parameters for three conformations of the tolane molecule and its positive and negative ions. These calculations have been performed with use of the B3PW91/6-311G** level of theory. The planar structure **1a** of D_{2h} point group and electronic state ^1A_g corresponds to the lowest energy configuration. This is followed by the D_2 structure **1b** where the phenyl rings are making an angle of 45°. The highest energy configuration is obtained when the two phenyl rings are perpendicular, **1c**, i.e., a D_{2d} structure with electronic state $^1A_1$. The rotational barrier for the phenyl rings is 0.86 kcal/mol. Table 1 also shows the corresponding positive and negative ion energies. As shown in Table 1, the rotational barriers for the positive and the negative ions are very large, 14 and 12 kcal/mol, respectively, with respect to the barrier for the neutral system. This can be explained because the ejection or absorption of an electron breaks the cylindrical structure of the electron density along the axis of symmetry. From the energies of the neutral and charged ions we can also compute the ionization potential (IP) and electron affinity (EA). The electron affinity is larger when the molecule is planar, and minimum (strongly negative, indicating a repulsive barrier for the electrons) when the phenyls are at 90° to each other. On the other hand, the ionization potential is very large for all structures. Therefore, based on the calculations shown in Table 1, we can infer that tolane prefers to be planar and has a small barrier to rotation of 0.86 kcal/mol. The conductivity on this molecule is achieved mainly by the molecule accepting one electron rather than donating one electron. In addition, the conductivity would be maximum when the phenyls are planar and minimum when the phenyls are perpendicular. We can also observe that the effects of relaxation are very large since the negative of the LUMO energy is five times larger than the electron affinity. Tolane would behave as a conductor with a variable conductivity controllable by the angle between the phenyls rings.

We also studied the intermolecular effects in tolane molecules. To test smaller levels of theory that will allow us to perform calculations on larger systems, we decided to investigate a well-studied system, the benzene dimer. Table 2 shows the results for the benzene dimer. The parallel sandwich **2a** is totally repulsive, meaning the optimization does not find a stationary point; however, a stationary point is found for the parallel-displaced structure **2b** and for the T-shaped structure **2c**. The lowest energy configuration corresponds to **2c**. The parallel displaced structure **2b** is very close in energy, at only 0.06 kcal/mol above **2c** with use of the best level of theory (B3PW91/6-311G**). These results indicate that benzene rings prefer to stay in a T-shape rather than in the sandwich conformation at least around 0 K. The LUMO energy is minimum in the T-shape structure **2c**, suggesting that the electron affinity is largest in **2c** and also is larger than in the isolated benzene by 34%. It only increases 13% in the parallel displaced form **2b**.

The five possible tolane dimers are shown in **3a**−**e**. It could be inferred from the analysis of these two systems, tolane and the benzene dimer, that the most stable structure for a tolane dimer would be one where both molecules are planar and one tolane is perpendicular to the adjacent tolane as in **3e**. It could also be inferred that structure **3e** has better conductivity than structure **3d** since the phenyl rings of the monomers in **3e** are planar and those in **3e** are perpendicular. To check these assumptions, we performed the calculations on the tolane dimer and the results were qualitatively correct but not quantitatively as expected.

DFT calculations tend to underestimate transition barriers.[27] For systems with weak interactions, this underestimation may be smaller than the activation barrier, therefore resulting in no

---

(22) Hay, P. J.; Wadt, W. R. *J. Chem. Phys.* **1985**, *82*, 299−310.

(23) Görling, A.; Levy, M. *J. Chem. Phys.* **1997**, *106*, 2675−2680.

(24) Frisch, M. J.; Trucks, G. W.; Schlegel, H. B.; Gill, P. M. W.; Johnson, B. G.; Robb, M. A.; Cheeseman, J. R.; Keith, T.; Petersson, G. A.; Montgomery, J. A.; Raghavachari, K.; Al-Laham, M. A.; Zakrzewski, V. G.; Ortiz, J. V.; Foresman, J. B.; Ciolowski, J.; Stefanov, B. B.; Nenayakkara, A.; Challacombe, M.; Peng, C. Y.; Ayala, P. Y.; Chen, W.; Wong, M. W.; Andres, J. L.; Replogle, E. S.; Gomperts, R.; Martin, R. L.; Fox, D. J.; Binkley, J. S.; Defrees, D. J.; Baker, J.; Stewart, J. P.; Head-Gordon, M.; Gonzalez, C.; Pople, J. A. *Gaussian 94*; E.1 version; Gaussian, Inc.: Pittsburgh, PA, 1996.

(25) Peng, C.; Ayala, P. Y.; Schlegel, H. B.; Frisch, M. J. *J. Comput. Chem.* **1996**, *17*, 49−56.

(26) Neyman, K. M.; Pacchioni, G.; Rösch, N. In *Recent Developments and Applications of Modern Density Functional Theory*; Seminario, J. M., Ed.; Elsevier: Amsterdam, 1996; pp 569−619.

(27) Jursic, B. S. In *Recent Developments and Applications of Modern Density Functional Theory*; Seminario, J. M., Ed.; Elsevier: Amsterdam, 1996; Vol. 4, pp 709−741.

Table 2. Optimized Geometries and Relative Energies for Benzene and Conformations of the Benzene Dimer (1 E_h = 627.509 kcal/mol)

	sandwich **2a** D_{6h} $^1A_{1g}$	parallel-displaced **2b** C_{2h} ^1A_g	T-shaped **2c** C_{2v} $^1A_1$	benzene D_{6h} $^1A_{1g}$
HF/3-21G				
distance (Å)	∞	2.9/5.0[a]	2.46	0.00
binding (kcal/mol)	0.00	−0.90	−1.11	−212.7
HOMO (kcal/mol)	−212.6	−210.4	−207.3	94.9
LUMO (kcal/mol)	95.0	92.2	91.6	
HF/6-31G*				
distance (Å)	∞	2.9/5.1[a]	2.46	0.00
binding (kcal/mol)	0.00	−0.62	−0.67	−207.4
HOMO (kcal/mol)	−207.4	−205.5	−203.6	93.9
LUMO (kcal/mol)	94.1	91.4	91.6	
B3PW91/6-31G*				
distance (Å)	7.1(∞)	5.4/3.2[a]	2.48	0.00
Binding (kcal/mol)	+0.16	+0.10	−0.33	−157.4
HOMO (kcal/mol)	−156.3	−156.2	−154.0	0.4
LUMO (kcal/mol)	1.5	1.4	−1.8	
B3PW91/6-311G**				
distance (Å)	13.9(∞)	6.1/3.9[a]	2.48	0.0
binding (kcal/mol)	+0.01	−0.20	−0.26	−163.0
HOMO (kcal/mol)	−162.8	−162.4	−159.4	−6.8
LUMO (kcal/mol)	−6.6	−7.7	−9.2	

[a] For *a*/*b* distances see **2b**.

Table 3. Optimized Geometries and Energies for Several Conformations of Tolane Dimer Molecule (1 E_h = 627.5095 kcal/mol)

	HF/3-21G	HF/6-31G*	B3PW91/6-31G*
3a: D_{2h} ^1A_g			
distance (Å)	15.3	17.6	
energy(kcal/mol)	2.7	1.6	
HOMO (kcal/mol)	−183.9	−180.0	
LUMO (kcal/mol)	55.3	57.1	
3b: D_{2h} ^1A_g			
distance (Å)	11.8		
energy(kcal/mol)	3.1		
HOMO (kcal/mol)	−185.5		
LUMO (kcal/mol)	53.7		
3c: C_s $^1A'$			
distance (Å)	26.9	28.1	
energy(kcal/mol)	3.5	2.4	
HOMO (kcal/mol)	−200.6	−195.9	
LUMO (kcal/mol)	71.7	72.8	
3d: C_s $^1A'$			
distance (Å)	5.0	5.4	5.5
energy(kcal/mol)	0.2	0.4	1.39
HOMO (kcal/mol)	−198.2	−194.0	−143.3
LUMO (kcal/mol)	69.7	71.3	−19.9
D_e (kcal/mol)			1.01
3e: C_{2v} $^1A_1$			
distance (Å)	5.3	5.6	5.7
energy(kcal/mol)	0.0	0.0	0.0
HOMO (kcal/mol)	−179.0	−176.1	−130.4
LUMO (kcal/mol)	50.8	53.9	−33.9
D_e (kcal/mol)			0.68
1a: D_{2h} ^1A_g			
HOMO (kcal/mol)	−184.3	−180.2	−134.0
LUMO (kcal/mol)	55.0	56.8	−31.4

Chart 1

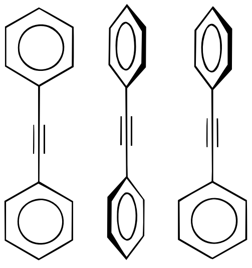

(**1a**) (**1b**) (**1c**)

Chart 2

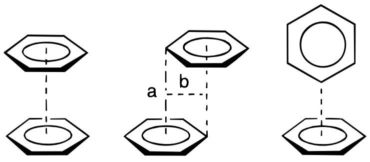

(**2a**) (**2b**) (**2c**)

binding. As a result of the small values of the interaction energy between phenyl rings, it may be that this interaction is lost due to the small activation barrier. This may be the case of the sandwich conformation of the benzene dimer; on the other hand, related studies indicate that other GGAs might yield better results for weakly bonded systems.[28,29] However, DFT calculations have been shown to predict correct relative energies and energy trends. In this respect, results are more precise than any of the standard ab initio calculations such as Møller−Plesset (MP), coupled cluster (CC), or configuration interaction (CI) techniques.[6] For instance, atomization energies are more accurate than any of the above methods when no empirical corrections are made.[6] The energy difference between the benzene dimer conformations T-shape and parallel displaced is in full agreement with the range of results obtained with MP2 (second-order MP), MP4 (fourth-order MP), and CCSD(T) (CC including single, double, and triple excited determinants) with basis sets as large as those having f-polarization functions.[30] On the other hand, the fact that the benzene dimer does not form a stable structure with DFT may be connected to the possibility that this is a transition state structure between two stable conformations of the dimer.[30] The calculation of weak transition state energies is still beyond the accuracy of present ab initio calculations.

Table 3 shows the results for the tolane dimer. We calculated the energies of the structures shown in Chart 1. By using lower levels of theory, configurations **3a**, **3b**, and **3c** were discarded

---

(28) Wesolowski, T. A.; Parisel, O.; Ellinger, Y.; Weber, J. *J. Phys. Chem. A* **1997**, *101*, 7818−7825.

(29) Patton, D. C.; Pederson, M. R. *Phys. Rev. A* **1997**, *56*, 2495−2498.

(30) Hobza, P.; Selzle, H. L.; Schlag, E. W. *J. Phys. Chem.* **1996**, *100*, 18790−18794.

Chart 3

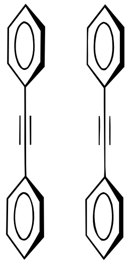

(**3a**)

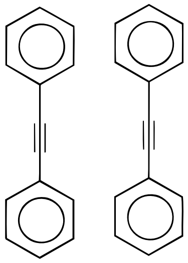

(**3b**)

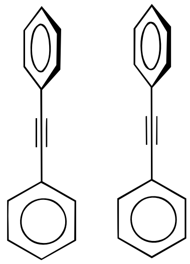

(**3c**)

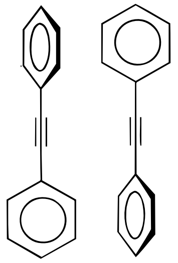

(**3d**)

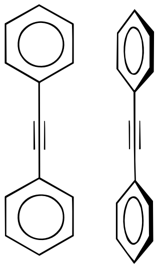

(**3e**)

and other possible structures not shown in Chart 3 were of no interest for this study. Only **3d** and **3e** remained as candidates for the lowest structure of the dimer. As expected from our study of the tolane monomer and the benzene dimer, structure **3e** is the lowest in energy. Structure **3d** is 1.39 kcal/mol higher in energy than the energy of **3e**. However, this energy is 0.33 kcal/mol lower than the tolane energy difference of **3d** and **3e** if they were infinitely separated from each other. It is expected that as the number of tolanes in a cluster of a SAM increases, this difference between the planar and perpendicular cluster will eventually reduce to zero because the tolane molecules bind better when they are in their perpendicular conformations. Such a difference is already very small at the HF level which, in general, provides reliable results for hydrocarbon conformations. Therefore, on the basis of these calculations, it is inferred that the clustering of perpendicular tolanes is going to compete with their planar counterparts, implying that clusters of perpendicular tolanes might eventually be more stable than clusters of parallel tolane molecules. If this is the case, the conductivity of the lowest energy clusters might be low with respect to the more energetic clusters. Therefore, at temperatures near 0 K, the conductivity of the full cluster is less than the conductivity of the cluster at higher temperatures. At higher temperatures, the rings in the tolane molecules are able to rotate, thereby allowing them to frequently approach the planar geometry. Experimental evidence indicates that the conductivity undergoes a sudden increase when the temperature of the SAM is increased to about 30 K.[4] This is reproduced by our molecular simulations of the tolane sandwich as explained below.

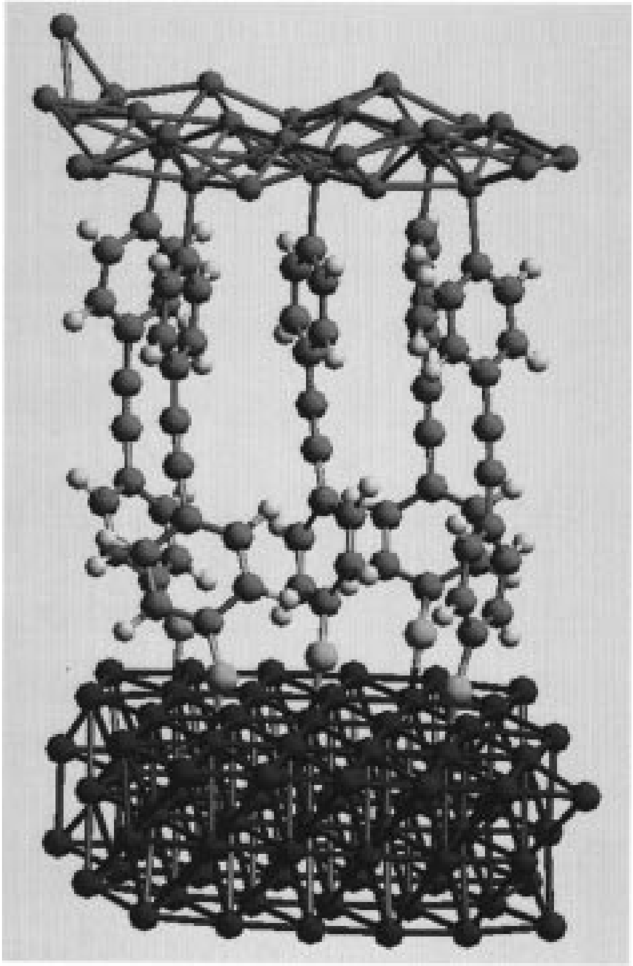

Figure 1. The Thiotolane Sandwich. The configuration contains one level of 21 Ti atoms (top), five thiotolane molecules in the middle with the thiolates projected downward and a Ti−aryl carbon bond on top, and three layers of 21 Au atoms each (bottom).

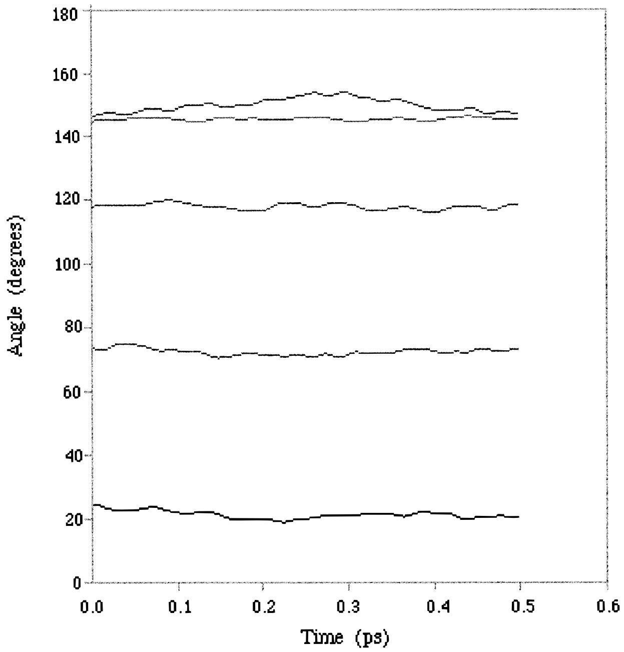

Figure 2. Variations of the angles between the two phenyl planes of each tolane molecule at 10 K.

The thiotolane SAM was modeled as indicated in Figure 1.[4] The gold and titanium surfaces were formed with layers of 22

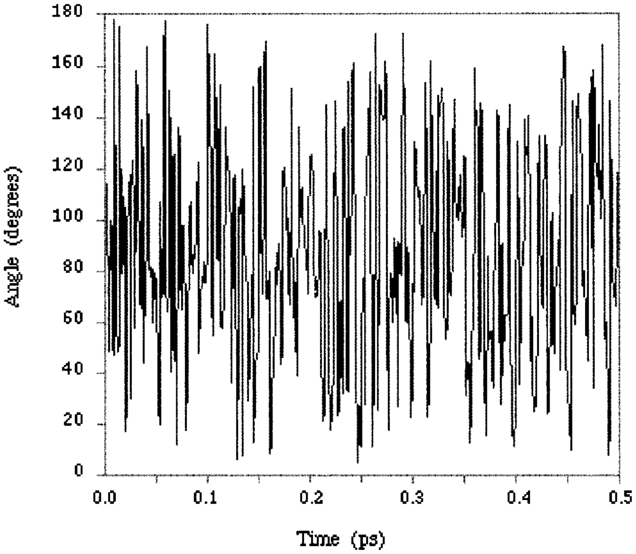

Figure 3. Variations of the angle between the two phenyl planes for one of the tolane molecules at 30 K.

atoms, with three layers for the gold (111) surface and one for the titanium (111) surface. This resembles the experimental setup except for the fact that the experiment used a surface of 300 Å per side and our simulation used a surface of 12 Å per side.[4] This system was minimized by using standard classical molecular mechanics in order to obtain an initial geometry. All simulations were made with a time step of 0.5 fs. Equilibration periods of 10 ps were used. The production runs were also in periods of 10 ps. The NVE microcanonical ensemble was used for all runs. Figure 2 shows the variations of the angle between the phenyl rings for the five tolane molecules in the sandwich at 10 K. At this temperature, the phenyl rings in the tolane molecules show very little tendency to rotate. However, Figure 3 shows the angle between the phenyl rings for one of the tolane molecules at 30 K. This result is also very similar for the other tolanes in the sandwich, indicating that the tolane rings are able to freely rotate with respect to each other.

We can conclude from these simulations, and the results of the DFT calculations, that at some temperature between 10 and 30 K, the rings in the tolane molecules start rotating, thereby allowing the tolane molecules to assume planar conformations. This permits the tolane molecules to reach a maximum of conductivity. However, between 0 K and ca. 10 K, a global clustering configuration ensues which has perpendicular phenyl rings within each of the tolane molecules. This causes a concomitant decrease in the conductivity which is in perfect agreement with the observed experimental results.[4] This work shows that, in addition to wire-like properties, this class of phenylene−ethynylene oligomers can behave as full current controllers because the electronic transport properties vary significantly based on the molecular conformations.

Acknowledgment. We thank Professor M. A. Reed and Mr. C. Zhou from Yale University for providing their results of conductivity measurements and Dr. M. J. Frisch of Lorentzian, Inc. We also thanks the Defense Advanced Research Projects Agency and the Office of Naval Research (N00014-97-1-0806) for support of this work. We acknowledge NASA for the use of their supercomputing facilities.

Supporting Information Available: The calculated energies (in hartrees) for Tables 1−3 (3 pages, print/PDF). See any current masthead page for ordering information and Web access instructions.

JA973639K